

Lightweight Residual Densely Connected Convolutional Neural Network

Fahimeh Fooladgar, and Shohreh Kasaei, *Senior Member, IEEE*
Department of Computer Engineering, Sharif University of Technology, Tehran, Iran

Extremely efficient convolutional neural network architectures are one of the most important requirements for limited computing power devices (such as embedded and mobile devices). Recently, some architectures have been proposed to overcome this limitation by considering specific hardware-software equipment. In this paper, the residual densely connected blocks are proposed to guaranty the deep supervision, efficient gradient flow, and feature reuse abilities of convolutional neural network. The proposed method decreases the cost of training and inference processes without using any special hardware-software equipment by just reducing the number of parameters and computational operations while achieving a feasible accuracy. Extensive experimental results demonstrate that the proposed architecture is more efficient than the AlexNet and VGGNet in terms of model size, required parameters, and even accuracy. The proposed model is evaluated on the ImageNet, MNIST, Fashion MNIST, SVHN, CIFAR-10, and CIFAR-100. It achieves state-of-the-art result on the Fashion MNIST dataset and reasonable results on the others. The obtained results show that the proposed model is superior to efficient models such as the SqueezeNet and is also comparable with the state-of-the-art efficient models such as CondenseNet and ShuffleNet.

Index Terms—Image Classification, Convolutional Neural Networks, Deep Learning, Efficient Architecture.

I. INTRODUCTION

IN the last decades, Convolutional Neural Networks (CNNs) have changed the landscape of visual recognition tasks such as image classification [1], [2], [3] and semantic segmentation [4], [5], [6]. These models need large training datasets with high-end GPU devices to learn a large number of parameters via a high number of computational operations. However, the most important issues in CNN models are the hardware and the burden of computational cost. Yet, complex CNNs [3] with high resource demands have been proposed to increase the accuracy. In addition, the ultra-deep CNN models have further increased the depth of networks from 8 layers (AlexNet) [7] to more than one thousand layers (ResNet) [1]. In fact, the general idea of CNNs has proceeded through deeper and more complex networks to boost the performance in terms of model's accuracy. But, the efficiency of networks in terms of model's size, inference speedup, and computational costs have been rarely inspected. For mobile and embedded devices (such as robotics, drones, and smartphones) the model size, runtime, memory requirement, inference time, and computational cost are very important. As such, a serious question which arises is whether it is really necessary to have these complex models with a huge number of parameters and computational operations.

The amount of redundancy among the parameterization of CNNs facilitates some novel pruning, quantization, and factorization methods to reduce the model size. Denil et al. [8] demonstrated this significant redundancy in the weights of neural networks. The efficiency of networks in the viewpoint of special purpose applications (like robotics, augmented realities, and self-driving cars) established some novel model structures with impressive architecture designs. ResNet [1], [2] and DenseNet [9] proposed two novel architectures which reduced the computational cost by a factor of $5\times$ and $10\times$ alongside boosting the accuracy when compared to the VGG

[10] on Imagenet dataset[7]. Meanwhile, the MobileNet [11], ShuffleNet [12], and CondenseNet [13] reduced the computational cost approximately by a factor of $25\times$, $25\times$, and $20\times$, respectively, while obtaining a comparable accuracy to the VGG on ImageNet.

The general notion of shortcut connection and residual connection have been proposed by the highway networks [14], [15] and ResNet model [1], [2], respectively. Thereafter, DenseNet [9] presented the idea of densely connected layers where each layer obtains concatenated feature maps of preceding layers. Subsequently, these two main ideas have been applied on different applications and network architectures. For instance, the skip connections have been exploited on encode-decoder models for dense prediction tasks (such as semantic segmentation and depth estimation) [16], [17]. The local and global residual connections have been utilized for image super-resolution and restoration via exploiting the hierarchical features from all preceding convolutional layers [18], [19]. These different models and applications have a share characteristic which create short paths from early layers to later ones via these two main concepts while they differ in network topology, training procedure and challenges.

In this paper, the idea of feature reuse ability of the DenseNet [9] with the residual connection idea of the ResNet [1] are exploited to achieve an ultra slimmed deep network. The proposed architecture, called Efficient Residual Densely Connected CNN (RDenseCNN), is illustrated in Figure 1. In the proposed method, an extremely small-size CNN model is presented to reduce the computational cost, memory requirement, and inference time without utilizing any new operation or hardware-software equipment. The performance of the proposed model is extensively evaluated on the ImageNet [7], MNIST [20], Fashion MNIST [21], SVHN [22], CIFAR-10, and CIFAR-100 [23] datasets. The obtained results show that its performance is comparable with most available networks in terms of the accuracy, number of parameters, and Floating

Point Operations (FLOPs). Our proposed method has obtained superior performance on MNIST, Fashion MNIST and CIFAR datasets. Moreover, the model has achieved a higher accuracy with $46\times$ smaller model size when compared to the AlexNet with $\%4.8$ higher in accuracy on ImageNet. It has also attained $2\times$ lower number of parameters at only $\%3$ drops in top-1 accuracy compared to the MobileNet [11].

Main contributions of this paper are as follows:

- Presenting an extremely small CNN model with feature reuse abilities, deep supervision, and efficient gradient flows by residual densely connected blocks.
- Reducing the computational cost and memory requirements with a feasible accuracy.
- Presenting a CNN model with basic common operations without requiring additional software or hardware equipment.
- Analyzing CNN models in terms of accuracy versus the number of parameters.
- Representing the effect of residual connections alongside the densely connected blocks (this can be an important result for those who want to combine these two ideas).

This paper is organized as follows. In Section II, the related work is explained in four categories. The proposed efficient residual densely connected CNN is introduced in Section III. Experimental results on six most import image classification datasets are reported in Section IV. In Section V and VI, concluding remarks are discussed.

II. RELATED WORK

The aim of designing efficient CNN architectures is to develop these models for limited resource devices. There are three main limitations for running CNN models on embedded devices; namely, the model size, the run-time memory requirement, and the required number of operations. Some methods have been proposed to overcome these constraints by compressing the model size in different ways. These can be classified into four main categories of: (i) quantizing and factorizing, (ii) pruning redundant connections, (iii) learning efficient architectures, and (iv) designing efficient architectures. These are explained next.

Quantizing and factorizing: To compress large CNN models, Denton et al. in [24] proposed to approximate the fully connected weights of CNNs by singular value decomposition methods. They obtained approximately $3\times$ compression in the model size. Weight quantization is another method to compress the model size. HashNet [25], Binarized Neural Networks [26], and Xnor-net [27] (binary or ternary weight quantizations) can also compress the model size, save run-time memory, and speed up the inference time, but to the cost of reduced accuracy.

Pruning and sparsifying: These methods can be performed at different granularity levels (weight, kernel, channel, and layer levels). In [28], unimportant connections with small weights were pruned to compress the model size and to save the memory. The authors of [29] and [30] proposed pruning at

kernel and neuron levels, respectively. Wen et al. [31] proposed to apply the sparsity at different levels of CNNs' structure (kernels, channels, and layers). All of these methods decreased the run-time memory and time elapse at a moderate accuracy loss. But, in some cases, they need special libraries to apply the pruning and sparsifying modules.

From the fine-to-coarse grains of pruning level, flexibility, generality, and compression ratio decrease. Meanwhile, special hardware/software requirements are needed for almost fine grain levels.

Designing efficient architectures: Recent CNN structures (such as the ResNet [1], DenseNet [9], and Xception [32]) have more efficient models than early CNNs (like AlexNet [7] and VGG [10]). In addition, specific purpose CNN models [13], [33], [11], [12] have been designed to decrease the computational cost and memory requirement with the speedup in inference time. To reduce the model size (number of parameters) and computational cost (number of Add-Multiplication operations), these CNN models utilized the idea of group convolution and depth-wise separable convolution. The extreme version of inception modules (called Xception) was proposed by Chollet [32] to boost the performance of the Inception V3 by substituting Inception modules with depth-wise separable convolutions. The MobileNet [11] proposed an efficient small architecture that applied the depth-wise convolution followed by the point-wise convolution as the depth-wise separable convolution to reduce the computational cost and model size. Howard et al. [11] proposed two hyper parameters as the width and resolution multipliers that controlled the input width of a layer and the input image resolution, respectively. The Channel shuffle was proposed to generalize the cascaded group convolutions. In other words, the ShuffleNet [12] reformed the group and depth-wise separable convolutions by shuffling the outputs of the point-wise group convolution fed to the depth-wise separable convolutions. The authors of CondenseNet [13] proposed to learn these groups at the training phase by a novel module called learned group convolution. At the half of training iterations, their network eliminated filters with small magnitude weights; hence the structure of convolution layers sparsified. Consequently, the kernel pruning performed as the condensation procedure by the condensation factor. In the second half of the training phase, fixed filters were trained. Then, at each layer, the index layer was proposed to select and rearrange the orders of input feature maps.

Learning efficient architectures: Some new methods proposed to learn the structure of networks, automatically. Baker et al. [34] proposed to learn the structure of CNNs by reinforcement learning. Network slimming [35] was another approach which tried to learn a scale factor for each layer to eliminate channels with small scaling factors. The authors of [35] considered the loss function with the L1-norm penalty on the scaling factors to apply sparsity. These approaches succeeded in dealing with all mentioned limitations, but they need iterative training procedures to train the slimmed network.

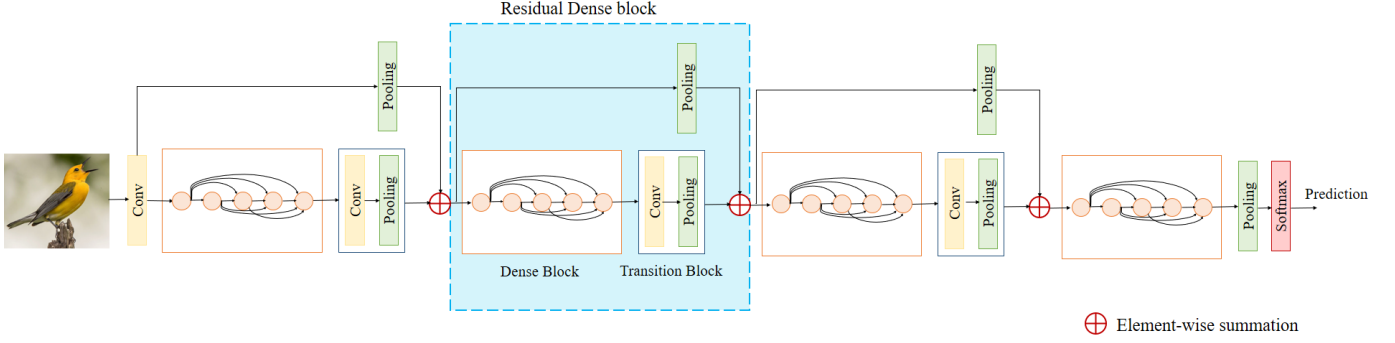


Fig. 1: Proposed RDenseCNN model with 4 dense blocks and 3 transition blocks.

III. PROPOSED EFFICIENT RESIDUAL DENSELY CONNECTED CNN

Novel CNN models are constructed as sequentially cascaded layers or basic blocks. Each layer l or basic block k can be denoted as a function $F_l(\cdot)$ or $H_k(\cdot)$, respectively. The output of the l^{th} layer or the k^{th} block is determined as x_l or y_k , accordingly. The $F_l(\cdot)$ function can be made from the compositions of some linear or non-linear functions; such as Convolution(Conv), Batch Normalization (BN), Rectified Linear Units (Relu), or Pooling (max or average pooling). The $H_k(\cdot)$ function can be formed by the combinations of functions that each of them belongs to each layer of the k^{th} block.

The proposed Residual Dense CNN is built upon the idea of residual and densely connected blocks. The common intention of DenseNet and ResNet is to reuse feature maps of preceding layers in the upper layers. Therefore, these two ideas are first elucidated. Then, the building block is clarified in detail.

Residual Blocks. Common CNN models have a plane structure in which the input of each intermediate layer comes directly from the output of the previous layer as $x_l = F(x_{l-1})$. But, in the residual block, the input goes through two different functions and the final output is the summation of their outputs, given by

$$x_l = F(x_{l-1}) + G(x_{l-1}). \quad (1)$$

The ResNet [1] proposed that the function G is an identity mapping $x_l = F(x_{l-1}) + x_{l-1}$. Therefore, it bypasses the non-linear transformations to resolve the vanishing gradient problem.

Densely Connected Blocks. In feed-forward networks, the output feature maps of each layer can be fed to all subsequent layers (as their input)

$$x_l = H([x_0, x_1, \dots, x_{l-1}]). \quad (2)$$

Then, all outputs of l preceding layers construct an input of the l^{th} layer, where $[.]$ denotes the concatenation of all previous feature maps as proposed by Huang et al. [9]. The equal size of feature maps is an essential factor for the concatenation

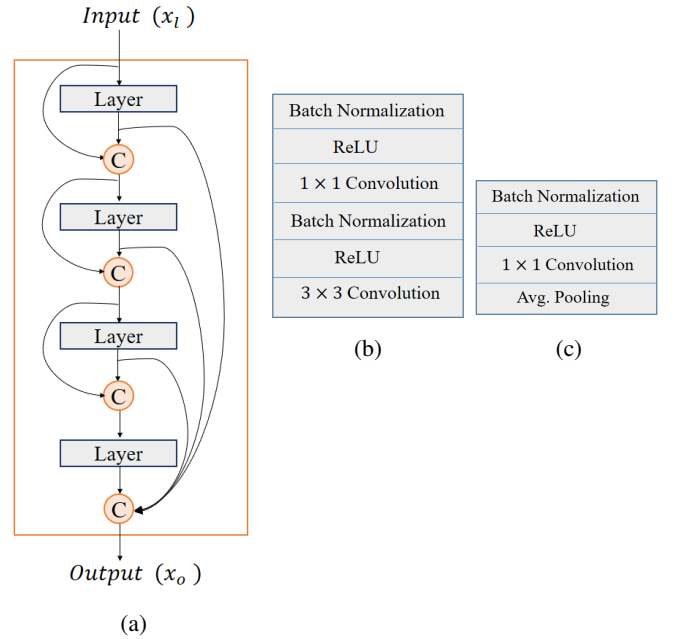


Fig. 2: Three building blocks: (a) dense block, (b) operations in each layer of dense block, (c) operations in transition block.

operation. The DenseNet [9] proposed densely connected blocks where the size of feature maps was preserved within each dense block. Therefore, the idea of densely connected CNNs can be applied locally within the range of layers in each block.

A. Details of Proposed Residual Densely Connected Model

The proposed method consists of the dense and transition blocks with one skip connection (see Figure 1). These combinations of non-linear transformations, performed in two consequent blocks, are bypassed by a skip connection. Suppose x_l is the input to the residual block, then the output of this residual block can be defined as

$$x_o = H(x_l) + F(x_l) \quad (3)$$

where $F(x_l)$ is utilized as a skip connection to ensure an unimpeded information flow through the network. The $H(x_l)$

TABLE I: Architectures for ImageNet. Each Conv. layer is denoted by BN-Relu-Conv. RDenseCNN-k-d ['k': growth rate, 'd': network depth].

Layers	Output size	RDenseCNN-k-132	RDenseCNN-k-160	RDenseCNN-k-200
Convolution	128×128	$4k, 3 \times 3 \text{ Conv}$		
Avg. Pooling	64×64	$2 \times 2 \text{ avg. pooling}$		
Dense Block-1	64×64	$\begin{bmatrix} 1 \times 1 \text{ Conv.} \\ 3 \times 3 \text{ Conv.} \end{bmatrix} \times 16$	$\begin{bmatrix} 1 \times 1 \text{ Conv.} \\ 3 \times 3 \text{ Conv.} \end{bmatrix} \times 20$	$\begin{bmatrix} 1 \times 1 \text{ Conv.} \\ 3 \times 3 \text{ Conv.} \end{bmatrix} \times 24$
Trans Block-1	32×32	$4k, 1 \times 1 \text{ Conv.}$ $2 \times 2 \text{ avg. pooling}$		
Dense Block-2	32×32	$\begin{bmatrix} 1 \times 1 \text{ Conv.} \\ 3 \times 3 \text{ Conv.} \end{bmatrix} \times 16$	$\begin{bmatrix} 1 \times 1 \text{ Conv.} \\ 3 \times 3 \text{ Conv.} \end{bmatrix} \times 20$	$\begin{bmatrix} 1 \times 1 \text{ Conv.} \\ 3 \times 3 \text{ Conv.} \end{bmatrix} \times 24$
Trans Block-2	16×16	$4k, 1 \times 1 \text{ Conv.}$ $2 \times 2 \text{ avg. pooling}$		
Dense Block-3	16×16	$\begin{bmatrix} 1 \times 1 \text{ Conv.} \\ 3 \times 3 \text{ Conv.} \end{bmatrix} \times 16$	$\begin{bmatrix} 1 \times 1 \text{ Conv.} \\ 3 \times 3 \text{ Conv.} \end{bmatrix} \times 20$	$\begin{bmatrix} 1 \times 1 \text{ Conv.} \\ 3 \times 3 \text{ Conv.} \end{bmatrix} \times 24$
Trans Block-3	8×8	$4k, 1 \times 1 \text{ Conv.}$ $2 \times 2 \text{ avg. pooling}$		
Dense Block-4	8×8	$\begin{bmatrix} 1 \times 1 \text{ Conv.} \\ 3 \times 3 \text{ Conv.} \end{bmatrix} \times 16$	$\begin{bmatrix} 1 \times 1 \text{ Conv.} \\ 3 \times 3 \text{ Conv.} \end{bmatrix} \times 20$	$\begin{bmatrix} 1 \times 1 \text{ Conv.} \\ 3 \times 3 \text{ Conv.} \end{bmatrix} \times 24$
Classification	1×1	$8 \times 8 \text{ Global avg. pool, } 1000 - D \text{ fc, softmax}$		

function is defined as

$$H(x_l) : H_T(H_D([x_l, x_{l+1}, \dots, x_{l+m}])) \quad (4)$$

where $x_{o-1} = H_D([x_l, x_{l+1}, \dots, x_{l+m}])$ denotes the non-linear transformations performed on outputs of m sequential densely connected layers of the dense block and x_{o-1} is an output of this dense block. The H_T indicates the non-linear functions performed in the transition block.

Composite function $H_D(\cdot)$. This function is a sequential combination of the BN, Relu, 1×1 Conv, BN, Relu, and 3×3 Conv defined as one layer of the dense block, as depicted in Figure 2. The overall structure of a dense block with 4 layers is illustrated in Figure 2.(a), where operations of each layer are given in Figure 2.(b).

Composite function $H_T(\cdot)$. This function is a sequential combination of the BN, Relu, 1×1 Conv, and 2×2 average pooling performed in the transition block depicted in Figure 2.(c). Hence, the spatial size of the output diminishes by a factor of 2 in each transition. Therefore, the element-wise summation of Equation (3) imposes a further down-sampling operation in the skip connection. To resolve the inconsistency of the size of the feature maps, the F in Equation (3) is considered to be an average pooling function instead of an identity map. However, F is a non-linear function and does not lead to loss of information about the original state of the image. Therefore, the input to the next block contains the down-sampled version of the original data; where it has been altered by the non-linearity function denoted by H .

Growth rate. Motivated by [9], each layer of the dense block produces k feature maps. Each dense block has m layers. Therefore, the output of the dense block has $(m-1) \times k + k_0$ feature maps, where k_0 is the number of input feature maps. The growth rate determines the amounts of new feature maps that each 3×3 convolution layer can exploit. Since the number of layers in each dense block is large, it is possible to limit the

growth rate. Consequently, the width of the proposed method can be managed and controlled.

B. Architecture Design

The proposed architecture is trained by a single end-to-end training procedure in contrast to some methods that need to be trained in two separate sequential training phases [13]. All operations of the RDenseCNN model are the basic CNN operations which are performed without requiring any special software or hardware to accelerate them. It has three architecture parameters of: (i) number of dense blocks, (ii) number of layers within each dense block, and (iii) growth rate. The network consists of only three or four dense blocks where each of them has 16, 20, or 24 layers. The growth rate (k) can be 12 or 16. The initial convolution layer has $4k$ convolution kernels of size 3×3 with stride and padding of 1. Hence, the number of convolutional kernels in the 1×1 convolution layer of the transition block is set to $4k$ to apply the element-wise summation of Equation (3). In Table I, the more details of three different configurations of RDenseCNN are illustrated.

IV. EXPERIMENTAL RESULTS

In this section, the effectiveness of the proposed RDenseCNN is evaluated in terms of computational cost, model size, and implementation requirements. It has been evaluated on six main datasets MNIST, Fashion-MNIST, SVHN, CIFAR-10, CIFAR-100, and ImageNet. The proposed model has been trained with different depths and growth rates. To compare the computational efficiency of the method, it has been compared with specific and general-purpose CNN models. It is implemented by using the PyTorch library. The code will be made publicly available on github.

A. Datasets

The following six important datasets, which are commonly used in the image classification have been employed to

evaluate the performance of the method.

MNIST. This database of handwritten digits [20] contains 60,000 and 10,000 examples as the training and test sets, respectively. The digits have been size-normalized and centered in 28×28 images.

Fashion MNIST (fMNIST). It can be seen as similar in flavor to MNIST (e.g., the image size and structure of training and testing splits) [21]. Each example is a 28×28 grayscale image corresponded to one of the 10 class labels.

Street View House Numbers (SVHN). It consists of over 600,000 images obtained from house numbers in Google Street View images [22]. The digit images are significantly more difficult to process compared to the MNIST examples as they are captured from real-world natural scenes.

CIFAR. It contains 60,000 colored low resolution 32×32 images with 10 and 100 classes, determined as CIFAR-10 and CIFAR-100 [23], accordingly. They contain 50,000 and 10,000 images for training and testing, respectively.

ImageNet. This is the pioneer large scale dataset for image classification [7]. It contains 1.2 million training and 50,000 validation images classified into 1000 classes.

B. Training Procedures

The proposed model was trained from scratch using the Stochastic Gradient Descent (SGD) optimization process. Mini-batch sizes were selected depending on the datasets. The mini-batch size was set to 64 and 30 for ImageNet dataset. It was set to 128 and 256 for five other datasets. The proposed model was trained during 120 and 300 epochs for the ImageNet and five other datasets, respectively. The training process was initialized with the learning rate of 0.1 and was decreased every 30 epochs by a factor of 10. The weight decay was set to 10^{-4} . Data augmentation methods for training images were utilized as in [9], [1].

C. Classification Results on MNSIT and Fashion-MNIST

One of the well-known benchmark datasets for machine learning algorithms is MNIST which most methods validate their algorithms based on it. The state-of-the-art accuracy in this dataset has been approached to %99.75. Hence, Xiao et al. [21] introduced Fashion-MNIST as a replacement of MNIST dataset in 2017. It includes 10 classes of "T-shirt, Trouser, Pullover, Dresser, Coat, Sandal, Shirt, Sneaker, Bag, and Ankle boot". Our network's inputs for both MNIST and Fashion-MNIST datasets are 28×28 grayscale images. The structure of RDenseCNN model is depicted in Table II. It contains three dense blocks alongside two transition blocks. The experiments were conducted on the smallest proposed model with $k = 12$ and $d = 100$. The performance of proposed method was compared with the most new CNN models which have validated their algorithm on MNIST and Fashion-MNIST datasets. The results are listed in Table III.

All available approaches that have published their results on these two datasets have not reported the number of parameters and floating-point operations. Therefore, it was not possible to compare the methods in terms of model size and computational complexity. But in terms of accuracy, the proposed method achieves the state-of-the-art results in Fashion-MNIST. Our proposed method attains %99.3 accuracy on Fashion-MNIST where it is %5.7 and %4 better accuracy than two recent models of CapsNet [36] and DENSER [37], respectively.

D. Classification Results on CIFAR and SVHN

The network inputs for both CIFAR and SVHN datasets were 32×32 images, with the per-pixel mean subtracted. The overall architectures considered for these two datasets were as those for the MNIST dataset which are depicted in Table II.

The experiments were performed on two different values of growth rate ($k=12$ and $k=16$) with three different network depths. They were compared with the most important special-purpose CNN models (such as the pruned version of CNNs and CondenseNet). As the results listed in Table IV shows, the proposed method has surpassed almost all of pruned CNN models. For instance, it obtained a lower classification error with $7 \times$ less number of parameters and approximately $2.3 \times$ fewer FLOPs than the VGG-pruned model [29], more especially in CIFAR-10. The RDenseCNN did not outperform the CondenseNet and pruned DenseNet-40 in terms of model size. But, note that it has lower computational cost with only %0.7 drops in the classification error. It is notable that the most recent efficient CNN models (like MobileNet and ShuffleNet) have not reported their performance on these two datasets.

In Table V, the classification error and the number of parameters are compared with the state-of-the-art CNN models. The RDenseCNN-152 has outperformed the VGGNet [10] and ResNet [1] models. ResNet and DenseNet models with a high number of parameters (more than 10M) have obtained a lower classification error in both CIFAR datasets. The proposed model has a comparable performance with DenseNet and ResNet models in terms of error and the number of parameters. CliqueNet [39] attained state-of-the-art classification error on SVHN but with 9.45G computational complexity while our proposed method has 121.4M FLOPS, approximately $80 \times$ lower computational complexity than CliqueNet.

E. Classification Results on ImageNet

The proposed method was evaluated on the ImageNet dataset. Figure 3 illustrates the behavior of RDenseCNN with different depths and growth rates. It shows top-1 and top-5 validation errors for two different RDenseCNN architectures during 120 epochs. The proposed model achieves lower top-1 and top-5 classification errors when the depth increases. The initial learning rate was set to 0.1 and decreased every 30 epoch. The comparison results with the state-of-the-art CNN models as well as efficient CNN architectures (designed for specific embedded devices) are shown in Figures 4 and 5. These two charts have been sorted based on top-1 accuracy. It provides a good intuition about the ratio of accuracy versus the model size. The overall architecture of the proposed method

TABLE II: Architectures for CIFAR datasets. Each Conv. layer is denoted as BN-Relu-Conv. RDenseCNN-k-d ['k': growth rate, 'd': network depth].

Layers	Output size	RDenseCNN-k-100	RDenseCNN-k-121	RDenseCNN-k-152
Convolution	32×32	$4k, 3 \times 3 \text{ Conv}$		
Avg. Pooling	16×16	$2 \times 2 \text{ avg. pooling}$		
Dense Block-1	16×16	$\begin{bmatrix} 1 \times 1 \text{ Conv.} \\ 3 \times 3 \text{ Conv.} \end{bmatrix} \times 16$	$\begin{bmatrix} 1 \times 1 \text{ Conv.} \\ 3 \times 3 \text{ Conv.} \end{bmatrix} \times 20$	$\begin{bmatrix} 1 \times 1 \text{ Conv.} \\ 3 \times 3 \text{ Conv.} \end{bmatrix} \times 24$
Trans Block-1	8×8	$4k, 1 \times 1 \text{ Conv.}$ $2 \times 2 \text{ avg. pooling}$		
Dense Block-2	8×8	$\begin{bmatrix} 1 \times 1 \text{ Conv.} \\ 3 \times 3 \text{ Conv.} \end{bmatrix} \times 16$	$\begin{bmatrix} 1 \times 1 \text{ Conv.} \\ 3 \times 3 \text{ Conv.} \end{bmatrix} \times 20$	$\begin{bmatrix} 1 \times 1 \text{ Conv.} \\ 3 \times 3 \text{ Conv.} \end{bmatrix} \times 24$
Trans Block-2	4×4	$4k, 1 \times 1 \text{ Conv.}$ $2 \times 2 \text{ avg. pooling}$		
Dense Block-3	4×4	$\begin{bmatrix} 1 \times 1 \text{ Conv.} \\ 3 \times 3 \text{ Conv.} \end{bmatrix} \times 16$	$\begin{bmatrix} 1 \times 1 \text{ Conv.} \\ 3 \times 3 \text{ Conv.} \end{bmatrix} \times 20$	$\begin{bmatrix} 1 \times 1 \text{ Conv.} \\ 3 \times 3 \text{ Conv.} \end{bmatrix} \times 24$
Classification	1×1	$4 \times 4 \text{ Global avg. pool, } 10 - D \text{ or } 100 - D \text{ fc, softmax}$		

TABLE III: Comparison of classification error (%) with state-of-the-art CNN models on MNIST and Fashion-MNIST(fMNIST) datasets.

Model	FLOPS	Params	MNIST	fMNIST
WRN-28-10 [38]	-	36.5M	-	4.1
WRN-28-10 + RE [38]	-	36.5M	-	3.7
CapsNet [36]	-	-	0.25	6.4
DENSER [37]	-	-	0.3	4.7
RDenseCNN-12-100	52.4M	0.61M	0.5	0.7

TABLE IV: Comparison of classification error (%) with efficient state-of-the-art CNNs on CIFAR-10(C-10) and CIFAR-100(C-100) datasets.

Model	FLOPs	Params	C-10	C-100
VGG-16-pruned [29]	206M	5.40M	6.60	25.3
VGG-19-pruned [35]	250M	5.0M	-	26.5
ResNet-56-pruned [29]	90M	0.73M	6.94	-
ResNet-110-pruned [29]	213M	1.68M	6.45	-
ResNet-164-B-pruned [35]	124M	1.2M	-	23.9
DenseNet-40-pruned [35]	190M	0.66M	5.19	-
CondenseNet-94 [13]	122M	0.33M	5.00	24.1
RDenseCNN-12-100	69.1M	0.61M	6.8	30.3
RDenseCNN-12-121	88.2M	0.78M	6.3	29.2
RDenseCNN-12-152	121.4M	1.1M	5.7	25.9

is depicted in Table I. The results presented in Figure 4 reveal that:

- RDenseCNN outperforms AlexNet in terms of both error rate and the number of parameters. It has $26\times$ lower number of parameters with 8 percent of higher accuracy.
- RDenseCNN has attained reasonable error rate by fewer number of parameters when compared with Inception V1, GoogleNet, and ResNet-18. It has approximately a $3\times$ smaller number of parameters at %3.4 drops in accuracy.
- The best model is Wide-ResNet-50 [42] which yields a %13 higher accuracy with a 66.6M additional number of parameters.

To show more details about these results, Figure 5 considers only more efficient models. The proposed RDenseCNN is more accurate than the SqueezeNet [33] even with fewer parameters. The method is also more efficient than some configurations of MobileNet (e.g., 0.25 MobileNet and 0.5 MobileNet). The MobileNet has width and resolution multipliers to design a smaller and faster model. The proposed

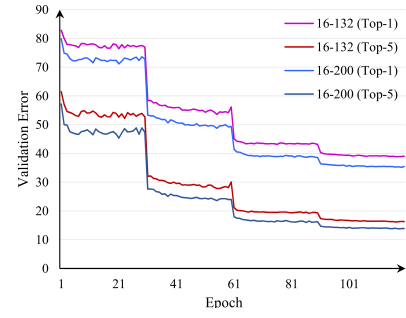


Fig. 3: Validation error for two RDenseCNN models.

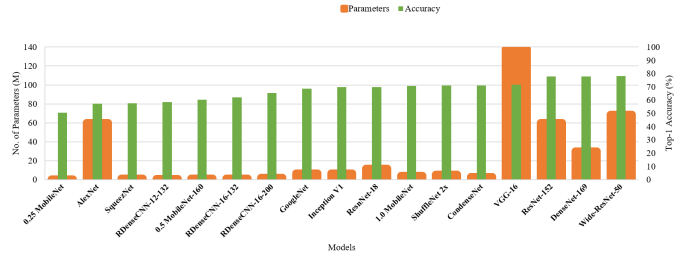


Fig. 4: Ratio of top-1 accuracy vs. number of parameters (models are evaluated on ImageNet dataset).

model has been compared with different configurations of the MobileNet. The results are listed in Table VI. These different configurations provide a trade-off between the classification error and the model size. At the same level of model size, RDenseCNN has achieved a very competitive classification error.

V. DISCUSSION

The proposed method evolved based on two well-known CNN models. The main goal of our architecture is to combine two ideas of these two models to achieve a more lightweight and efficient model. In other words, the proposed model is not an extension of DenseNet or ResNet model, it is a novel architecture that utilizes the residual and dense connection ideas with the light CNN structure. Our proposed model has less number of parameters and computational complexity at

TABLE V: Comparison of classification error (%) with state-of-the-art CNN models on CIFAR-10(C-10), CIFAR-100(C-100), and SVHN datasets. [‘+’ was reported in [35].]

Model	FLOPS	Params	C-10	C-100	SVHN
CapsNet [36]	-	-	10.6	-	4.3
SkipNet-ResNet110 [40]	-	-	6.4	28.8	1.9
CMPE-SE-WRN-28-10 [41]	-	36.9M	3.6	18.5	1.59
Wide ResNet-28-10 [42]	-	36.5M	4.0	19.3	-
DenseNet-24-100 [9]	-	27.2M	3.7	19.3	1.59
VGGNet[10]	-	20.0M ⁺	6.3 ⁺	26.7 ⁺	-
ResNet-1001 [2]	-	10.2M	4.6	22.7	-
CliqueNet [39]	9.45G	10.14M	5.06	23.14	1.51
ResNet reported by [43]	-	1.70M	6.4	27.2	2.0
ResNet-164 [2]	-	1.70M	5.5	24.3	-
ResNet with Stochastic Depth [43]	-	1.70M	5.2	24.6	1.8
RDenseCNN-12-152	121.4M	1.10M	5.7	25.9	2.5

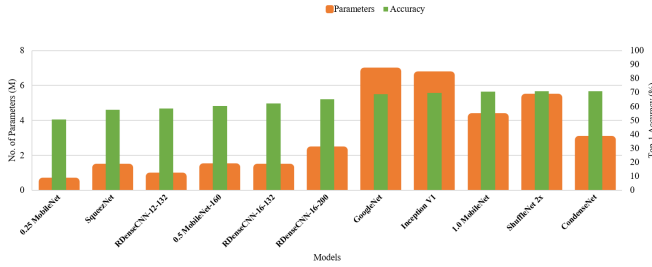


Fig. 5: Ratio of top-1 accuracy vs. number of parameters (efficient models are evaluated on ImageNet dataset).

TABLE VI: Comparison with different configurations of MobileNet [11] on ImageNet dataset.

Model	Params	Top-1 Error
1.0 MobileNet-224	4.2M	29.4
1.0 MobileNet-128	4.2M	35.6
0.75 MobileNet-224	2.6M	31.6
0.5 MobileNet-224	1.3M	36.3
0.5 MobileNet-160	1.3M	39.8
0.25 MobileNet-224	0.5M	49.4
RDenseCNN-12-132	0.8M	41.5
RDenseCNN-16-132	1.3M	38
RDenseCNN-16-200	2.3M	34.7

the level of feasible and comparable accuracy via the residual and dense connection ideas.

A. The Effect of Residual Connections

In this section, the importance of skip connection in each residual dense block is investigated. The proposed architecture without the skip connection is considered as “Plane-DenseCNN” (PDenseCNN). In this plane architecture, every dense block is connected in a sequentially cascaded manner. It is notable that this PDenseCNN is our lightweight model without residual connections and it is not a version of the well-known DenseNet model. To demonstrate the effectiveness of skip connections in the proposal residual dense block, two models have been evaluated on three datasets. Figure 6 compares the PDenseCNN and RDenseCNN models in terms of top-1 accuracy during training in both train and validation splits of datasets. The results presented in this figure reveal that the RDenseCNN performs more accurate than the

PDenseCNN. It attains approximately a %20 higher top1-accuracy whilst requiring the same number of parameters. This is because the residual connections do not enforce any additional number of parameters in our model. These experiments were performed based on the PDenseCNN-12-100 and RDenseCNN-12-100 models with 0.6M parameters.

B. Model Analysis

The efficient flow of gradients, feature reuse ability, and deep supervision in short and long ranges are three main properties of the proposed model. In each layer of the dense block, a small set of feature maps (based on the growth rate) is selected as the nonlinear composition of input feature maps. Then, these feature maps are concatenated with the previous ones and passed to the proceeding layer to produce the new nonlinear composition. In other words, the feature maps of early layers of each dense block can be reused by the last ones in the same dense block. This feature reuse ability preserves the information flows through two consecutive dense and corresponding transition blocks. In other direction, the skip connection utilized in each residual dense block amend the main information flows of the network. Meanwhile, the deep supervision was applied in the network by both dense connections in the residual block (short ranges) and also the skip connection (long ranges). In the densely connected model, each layer receives additional supervision from the loss function via a shorter connection. Hence, feature maps of intermediate layers learn more discriminative features.

The accuracy versus the number of parameters can be more informative for selecting an appropriate model based on requirements of specific applications to analyze the efficiency of CNN models. Therefore, the ratio of top-1 accuracy versus the number of parameters was computed for state-of-the-art CNN models. These are depicted in Figure 4. As shown in this figure, the RDenseCNN achieves the admissible rank among different state-of-the-art models based on these two evaluation metrics. The VGG-16, Wide ResNet and AlexNet have a significantly large number of parameters.

VI. CONCLUSION

One of the main goals of this work was to design an ultra-small model to analyze the amount of complexity of

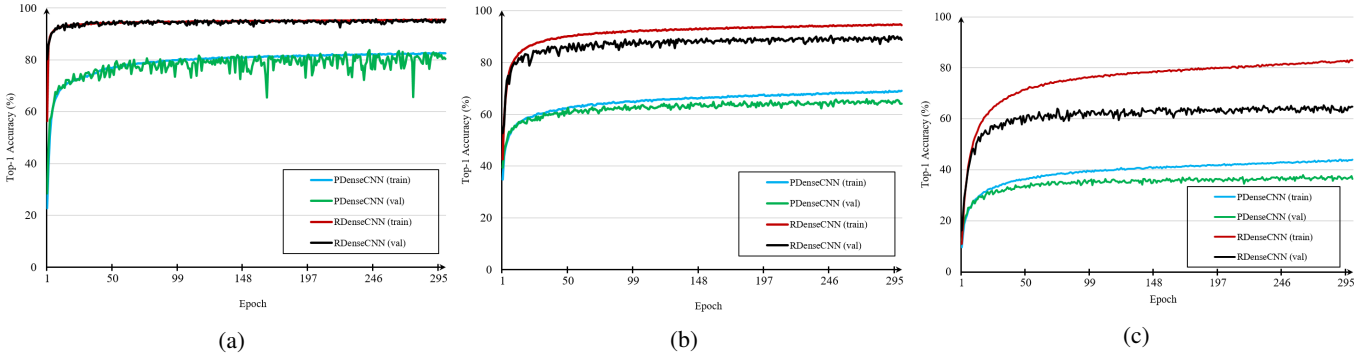


Fig. 6: Comparison of Plane-DesneNet and Residual-DenseNet on three datasets: (a) SVHN, (b) CIFAR-10, (c) CIFAR-100.

novel CNN architectures which have attained the state-of-the-art performance in terms of classification error. Towards this goal, a small CNN model was proposed based on two main ideas of residual connections and densely connected convolutional layers. This proposed RDenseCNN architecture had a few numbers of parameters with a feasible classification error. It contained densely connected layers in terms of some dense blocks with skip connections to preserve the flow of information in a deep CNN model. The proposed model had $26\times$ fewer number of parameters than the first widespread CNN model (AlexNet) with a %8 higher classification error. It is worth mentioning that the smallest proposed model had the same level of accuracy (%1 better accuracy) with the AlexNet at $60\times$ smaller model size. The results revealed that some levels of complexity in CNN models have unacceptable justifications, seriously in early CNN models. Consequently, these unfeasible complex models can be substituted by a significantly smaller and more efficient model, particularly in limited resource applications.

REFERENCES

- [1] K. He, X. Zhang, S. Ren, and J. Sun, "Deep residual learning for image recognition," in *Proceedings of the IEEE conference on computer vision and pattern recognition*, 2016, pp. 770–778.
- [2] —, "Identity mappings in deep residual networks," in *European conference on computer vision*. Springer, 2016, pp. 630–645.
- [3] J. Hu, L. Shen, and G. Sun, "Squeeze-and-excitation networks," in *Proceedings of the IEEE conference on computer vision and pattern recognition*, 2018, pp. 7132–7141.
- [4] M. Naseer, S. H. Khan, and F. Porikli, "Indoor scene understanding in 2.5/3d: A survey," *arXiv preprint arXiv:1803.03352*, 2018.
- [5] J. Long, E. Shelhamer, and T. Darrell, "Fully convolutional networks for semantic segmentation," in *Proceedings of the IEEE conference on computer vision and pattern recognition*, 2015, pp. 3431–3440.
- [6] F. Fooladgar and S. Kasaei, "A survey on indoor rgb-d semantic segmentation: from hand-crafted features to deep convolutional neural networks," *Multimedia Tools and Applications*, pp. 1–26, 2019.
- [7] A. Krizhevsky, I. Sutskever, and G. E. Hinton, "Imagenet classification with deep convolutional neural networks," in *Advances in neural information processing systems*, 2012, pp. 1097–1105.
- [8] M. Denil, B. Shakibi, L. Dinh, N. De Freitas *et al.*, "Predicting parameters in deep learning," in *Advances in neural information processing systems*, 2013, pp. 2148–2156.
- [9] G. Huang, Z. Liu, L. Van Der Maaten, and K. Q. Weinberger, "Densely connected convolutional networks," in *Proceedings of the IEEE conference on computer vision and pattern recognition*, vol. 1, no. 2, 2017, p. 3.
- [10] K. Simonyan and A. Zisserman, "Very deep convolutional networks for large-scale image recognition," *arXiv preprint arXiv:1409.1556*, 2014.
- [11] A. G. Howard, M. Zhu, B. Chen, D. Kalenichenko, W. Wang, T. Weyand, M. Andreetto, and H. Adam, "Mobilenets: Efficient convolutional neural networks for mobile vision applications," *arXiv preprint arXiv:1704.04861*, 2017.
- [12] X. Zhang, X. Zhou, M. Lin, and J. Sun, "Shufflenet: An extremely efficient convolutional neural network for mobile devices," in *Proceedings of the IEEE Conference on Computer Vision and Pattern Recognition*, 2018, pp. 6848–6856.
- [13] G. Huang, S. Liu, L. Van der Maaten, and K. Q. Weinberger, "Condensenet: An efficient densenet using learned group convolutions," in *Proceedings of the IEEE Conference on Computer Vision and Pattern Recognition*, 2018, pp. 2752–2761.
- [14] R. K. Srivastava, K. Greff, and J. Schmidhuber, "Highway networks," *arXiv preprint arXiv:1505.00387*, 2015.
- [15] —, "Training very deep networks," in *Advances in neural information processing systems*, 2015, pp. 2377–2385.
- [16] F. Fooladgar and S. Kasaei, "3m2rnet: Multi-modal multi-resolution refinement network for semantic segmentation," in *Science and Information Conference*. Springer, 2019, pp. 544–557.
- [17] D. Eigen and R. Fergus, "Predicting depth, surface normals and semantic labels with a common multi-scale convolutional architecture," in *Proceedings of the IEEE international conference on computer vision*, 2015, pp. 2650–2658.
- [18] Y. Zhang, Y. Tian, Y. Kong, B. Zhong, and Y. Fu, "Residual dense network for image super-resolution," in *Proceedings of the IEEE Conference on Computer Vision and Pattern Recognition*, 2018, pp. 2472–2481.
- [19] —, "Residual dense network for image restoration," *arXiv preprint arXiv:1812.10477*, 2018.
- [20] L. Deng, "The mnist database of handwritten digit images for machine learning research [best of the web]," *IEEE Signal Processing Magazine*, vol. 29, no. 6, pp. 141–142, 2012.
- [21] H. Xiao, K. Rasul, and R. Vollgraf, "(2017) Fashion-mnist: a novel image dataset for benchmarking machine learning algorithms."
- [22] Y. Netzer, T. Wang, A. Coates, A. Bissacco, B. Wu, and A. Y. Ng, "Reading digits in natural images with unsupervised feature learning," 2011.
- [23] A. Krizhevsky and G. Hinton, "Learning multiple layers of features from tiny images," Citeseer, Tech. Rep., 2009.
- [24] E. L. Denton, W. Zaremba, J. Bruna, Y. LeCun, and R. Fergus, "Exploiting linear structure within convolutional networks for efficient evaluation," in *Advances in neural information processing systems*, 2014, pp. 1269–1277.
- [25] W. Chen, J. Wilson, S. Tyree, K. Weinberger, and Y. Chen, "Compressing neural networks with the hashing trick," in *International Conference on Machine Learning*, 2015, pp. 2285–2294.
- [26] M. Courbariaux, I. Hubara, D. Soudry, R. El-Yaniv, and Y. Bengio, "Binarized neural networks: Training deep neural networks with weights and activations constrained to+ 1 or-1," *arXiv preprint arXiv:1602.02830*, 2016.
- [27] M. Rastegari, V. Ordonez, J. Redmon, and A. Farhadi, "Xnor-net: Imagenet classification using binary convolutional neural networks," in *European Conference on Computer Vision*. Springer, 2016, pp. 525–542.
- [28] S. Han, J. Pool, J. Tran, and W. Dally, "Learning both weights and connections for efficient neural network," in *Advances in neural information processing systems*, 2015, pp. 1135–1143.

- [29] H. Li, A. Kadav, I. Durdanovic, H. Samet, and H. P. Graf, "Pruning filters for efficient convnets," *arXiv preprint arXiv:1608.08710*, 2016.
- [30] H. Zhou, J. M. Alvarez, and F. Porikli, "Less is more: Towards compact cnns," in *European Conference on Computer Vision*. Springer, 2016, pp. 662–677.
- [31] W. Wen, C. Wu, Y. Wang, Y. Chen, and H. Li, "Learning structured sparsity in deep neural networks," in *Advances in neural information processing systems*, 2016, pp. 2074–2082.
- [32] F. Chollet, "Xception: Deep learning with depthwise separable convolutions," in *Proceedings of the IEEE conference on computer vision and pattern recognition*, 2017, pp. 1251–1258.
- [33] F. N. Iandola, S. Han, M. W. Moskewicz, K. Ashraf, W. J. Dally, and K. Keutzer, "Squeezenet: Alexnet-level accuracy with 50x fewer parameters and 0.5 mb model size," *arXiv preprint arXiv:1602.07360*, 2016.
- [34] B. Baker, O. Gupta, N. Naik, and R. Raskar, "Designing neural network architectures using reinforcement learning," *arXiv preprint arXiv:1611.02167*, 2016.
- [35] Z. Liu, J. Li, Z. Shen, G. Huang, S. Yan, and C. Zhang, "Learning efficient convolutional networks through network slimming," in *Proceedings of the IEEE International Conference on Computer Vision*, 2017, pp. 2736–2744.
- [36] S. Sabour, N. Frosst, and G. E. Hinton, "Dynamic routing between capsules," in *Advances in neural information processing systems*, 2017, pp. 3856–3866.
- [37] F. Assunção, N. Lourenço, P. Machado, and B. Ribeiro, "Denser: deep evolutionary network structured representation," *Genetic Programming and Evolvable Machines*, vol. 20, no. 1, pp. 5–35, 2019.
- [38] Z. Zhong, L. Zheng, G. Kang, S. Li, and Y. Yang, "Random erasing data augmentation," *arXiv preprint arXiv:1708.04896*, 2017.
- [39] Y. Yang, Z. Zhong, T. Shen, and Z. Lin, "Convolutional neural networks with alternately updated clique," in *Proceedings of the IEEE Conference on Computer Vision and Pattern Recognition*, 2018, pp. 2413–2422.
- [40] X. Wang, F. Yu, Z.-Y. Dou, T. Darrell, and J. E. Gonzalez, "Skipnet: Learning dynamic routing in convolutional networks," in *Proceedings of the European Conference on Computer Vision (ECCV)*, 2018, pp. 409–424.
- [41] Y. Hu, G. Wen, M. Luo, and D. Dai, "Competitive inner-imaging squeeze and excitation for residual network," *arXiv preprint arXiv:1807.08920*, 2018.
- [42] S. Zagoruyko and N. Komodakis, "Wide residual networks," *arXiv preprint arXiv:1605.07146*, 2016.
- [43] G. Huang, Y. Sun, Z. Liu, D. Sedra, and K. Q. Weinberger, "Deep networks with stochastic depth," in *European conference on computer vision*. Springer, 2016, pp. 646–661.